Highlight Review

Molecular Structures on Solid Substrates Probed by Sum Frequency Generation (SFG) Vibration Spectroscopy

Shen Ye and Masatoshi Osawa*

(Received January 8, 2009; CL-098001)

Abstract

Sum frequency generation (SFG) vibration spectroscopy is a powerful tool to study interfacial structures of organic thin films on solid substrates at a molecular level. The unique structural information obtained from SFG is essential to design and control functionalities of surfaces and interfaces. Recent advances in SFG spectroscopy are reviewed.

♦ Introduction

It is well known that surfaces or interfaces of materials have properties and functionalities considerably different from those of the bulk and are largely affected by their structures. The structural elucidation of the surface/interface at a molecular level under in situ conditions is becoming more and more important in both fundamental and applied research. Many modern surface analytical techniques, such as scanning probe microscopy (STM and AFM) and surface X-ray scattering (SXS), have been employed to investigate atomic and molecular arrangements on solid surfaces. However, difficulties are often encountered in analyzing the molecular structures in detail because they do not have enough molecular specificity and resolution. In this regard, vibrational spectroscopy that can provide abundant information about molecular structures is more suited for this purpose. Unfortunately, traditional vibrational spectroscopy techniques, such as infrared (IR) spectroscopy and Raman scattering, are not intrinsically surface-specific and usually not sensitive enough to study monolayers (especially on transparent and semitransparent materials). Surface-enhanced Raman scattering (SERS)[1] and surface-enhanced IR absorption spectroscopy (SEIRAS)[2] have very high sensitivities but are applicable only to metallic surfaces.

Sum frequency generation (SFG) spectroscopy is a second-order nonlinear optical technique that allows us to obtain vibrational spectra at surfaces and interfaces. SFG is generated by two laser photons at frequencies of ω_1 and ω_2 and observed as a single photon with a sum frequency at $\omega_3 = \omega_1 + \omega_2$.[3] For observing vibrational spectra, one of the frequencies is fixed in the visible (ω_{vis}), and the other is usually scanned in the infrared region (ω_{IR}). When ω_{IR} is equal to a vibrational level of the molecule, the SFG signal is resonantly enhanced (Figure 1). SFG can be further enhanced when ω_{vis} and/or ω_{SFG} are also resonant with an existing surface electronic state.

A SFG spectrum is given by

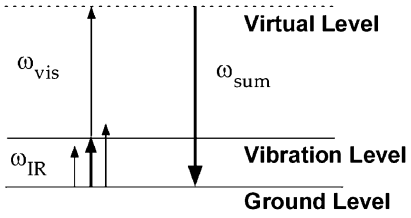

Figure 1. Energy diagram for sum frequency photon (ω_{sum}) generated from a tunable ω_{IR} photon and a fixed ω_{vis} photon.

$$I_{SFG} \propto \left| \sum_{\upsilon} \chi^{(2)}_{R,\upsilon} + \chi^{(2)}_{NR} \right|^2 = \left| \sum_{\upsilon} \frac{A_\upsilon}{\omega_{IR} - \omega_\upsilon + i\Gamma_\upsilon} e^{i\phi_\upsilon} + \chi^{(2)}_{NR} \right|^2 \quad (1)$$

where $\chi_{R,\upsilon}{}^{(2)}$ and $\chi_{NR}{}^{(2)}$ are second-order nonlinear susceptibilities corresponding to the resonant and nonresonant components, respectively. A_υ and Γ_υ are the amplitude and the damping constant, respectively, of the vibrational mode υ at a frequency ω_υ. ϕ_υ is the phase angle between the resonance mode and nonresonant background and significantly affects the shape of the SFG spectra when the nonresonant background is large.

SFG does not occur in homogenous media with symmetry of inversion under electric dipole approximation and is active only at the surface or interface where symmetry of inversion is broken. SFG has attracted much attention in recent years in multidisciplinary research fields, including electrochemical surface science, materials chemistry, and biophysics, because of its high surface selectivity, sensitivity, and versatile applicability. A great deal of valuable information at gas/solid, air/liquid, liquid/solid, and liquid/liquid interfaces has been reported, as has been reviewed in several reviews.[3–10] In this manuscript, molecular structures at buried interfaces, that were not covered so much in the previous reviews, are mainly focused, and then some applications of SFG on biointerface research including our recent results are reviewed.

♦ Experimental Setup

Two types of SFG systems are available at present: scanning systems using picosecond (ps) or nanosecond (ns) IR pulses and broad band systems using femtosecond (fs) IR pulse.[11] SFG measurements using ps or ns IR pulses can be done by scanning ω_{IR} while keeping ω_{vis} constant. The bandwidth of the ps IR pulse is several cm^{-1} and narrow enough for most spectral meas-

Dr. Shen Ye,[1,2] *Prof. Masatoshi Osawa*[1]
[1]*Catalysis Research Center, Hokkaido University, Sapporo 001-0021*
[2]*PRESTO, Japan Science and Techynology Agency (JST)*
E-mail: ye@cat.hokudai.ac.jp, osawam@cat.hokudai.ac.jp

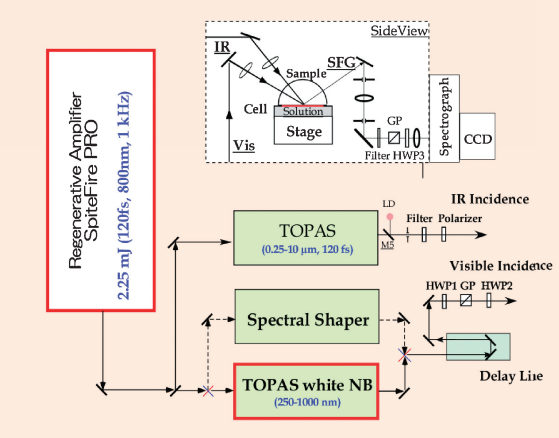

Figure 2. Schematic diagram of the broad-band double-resonance SFG system built in our group.

urements. On the other hand, the bandwidth of the fs pulse is much broader owing to the uncertainty principle. For example, a 100 fs pulse has a bandwidth wider than 250 cm^{-1} (FWHM). Accordingly, a SFG spectrum of this spectral width can be obtained at once. In order to have enough spectral resolution, however, a narrow-band ps visible pulse has to be used for the vibrational SFG spectroscopy. The latter system, normally called a broad-band SFG, has advantages in spectral acquisition time and S/N ratio over the scanning ps or ns system.

Figure 2 shows the broad-band fs SFG system with all-solid lasers built in our laboratory.[12–14] A Ti:sapphire fs laser oscillator (MaiTai) and a regenerative amplifier (SpiteFire PRO) pumped by a Nd:YLF laser (EMPower) can generate a 2.2 mJ pulse at 800 nm with a 120 fs duration at a repetition rate of 1 kHz. Half of the output was used to pump an optical parametric amplifier (OPA) system (TOPAS) to generate IR pulses tunable from 2.5 to 10 μm with a spectral width of ca. 250 cm^{-1}. Remaining output from the amplifier was sent to a home-made spectral shaper to generate a narrow-band pulse (ca. 10 cm^{-1}) at 800 nm for improving the spectral resolution. Tunable visible pulse output from the UV to near IR region (250–1000 nm) with a typical spectral width of ca. 20 cm^{-1} is available by using a narrow-band OPA (TOPAS white-NB). By making both ω_{IR} and ω_{vis} tunable, we were able to get enhanced SFG spectra under double-resonance conditions.

The broad-band fs IR pulse and the narrow-band visible pulse were overlapped on the sample surface with incident angles of 50 and 70°, respectively. Vibrationally resolved SFG spectra were acquired with a CCD detector attached to a spectrograph.[12–14]

Different polarization combinations of SFG, visible and IR beams can be used in SFG. They are represented, for example, as ssp-polarization, which indicates a combination of s-polarized SFG, s-polarized visible, and p-polarized IR. Molecular orientations can be discussed quantitatively from SFG spectra with different polarization combinations.[4–10,15]

♦ Results and Discussion

Buried Hetero-interfaces

It is well established that SFG is generated at the surface, but

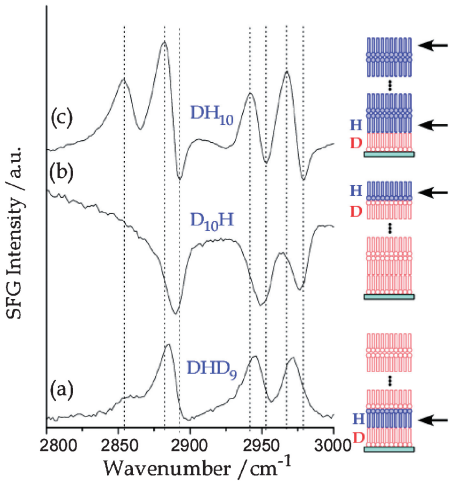

Figure 3. SFG spectra of arachidate LB multilayers with different structures on gold substrates. The polarization combination was ppp. The H layers that give SFG signals in the C–H stretching region are shown by arrows. See text for details. Reprint with permission from ref 15, Copyright American Chemical Society.

we should note that buried hetero interfaces also can be probed by SFG. Figure 3 shows SFG spectra in the C–H stretching region (2800–3000 cm^{-1}) for *Langmuir–Blodgett* (LB) films of arachidate on gold substrates having different layered structures of DHD_9 (a), $D_{10}H$ (b), and DH_{10} (c), where H and D stand for perprotonated and per-deuterated arachidate monolayers, respectively (total 11 layers).[16] The SFG spectrum of $D_{10}H$ (b) gives three peaks at 2880, 2940, and 2968 cm^{-1}, assignable to the symmetric Fermi resonance and asymmetric C–H stretching resonances, respectively, of the terminal CH_3 groups in the topmost H layer. No peaks from CH_2 groups can be observed, indicating that all CH_2 groups are in a local centrosymmetric environment; that is, the alkyl chains have all-trans conformation and are well ordered. The buried H layer in the DHD_9 also gives the corresponding peaks on spectrum (a). The slight shifts in peak frequency on the spectra may reflect the difference in chemical environments of the topmost and buried H layers. The weak CH_2 vibration at 2850 cm^{-1} indicates that the molecular arrangement in the buried H layer is slightly distorted.

An important finding in the figure is that the SFG spectra are greatly affected by molecular orientations. The CH vibrations of the buried H layer (a), in which CH_3 groups are directed toward the surface, gives positive peaks, while the topmost H layer with the opposite orientation gives negative peaks (b). On the other hand, the film (c) has two SFG-active interfaces (i.e., top air/H and bottom H/D interfaces) and hence gives the derivative-like features that can be given by the sum of spectra (a) and (b).

The inversion of peaks arises from the interference between resonant molecular vibrations and the nonresonant background from the substrate through the phase difference ϕ_v in eq 1.[16] This is evidenced by the fact that only upward SFG peaks are observed on other substrates that have weak nonresonance background (such as fused quartz and CaF_2). The ability to determine the absolute orientation is an advantage of SFG over conventional vibration spectroscopy and has been successfully used to determine the orientation of water molecules at water–air interface.[9]

Published on the web (Advance View) March 28, 2009; doi:10.1246/cl.2009.386

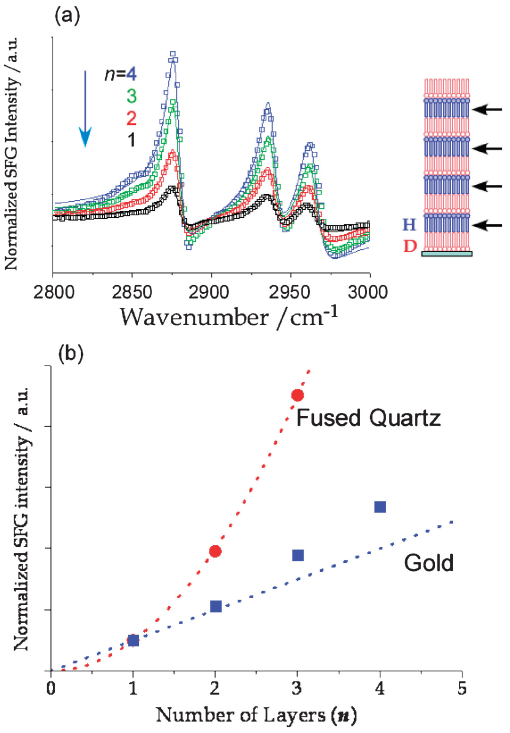

Figure 4. (a) SFG spectra of arachidate LB multilayers with different structures of $(DH)_n(DD)_mD$ on gold substrates as a function of the numbers of HD interfaces n. (b) Normalized SFG intensities of CH_3 group of the LB multilayers on gold (square) and fused quartz (circles) substrates. The lines in the figure are for eye guidance. Reprint with permission from ref 16, Copyright American Physics Society.

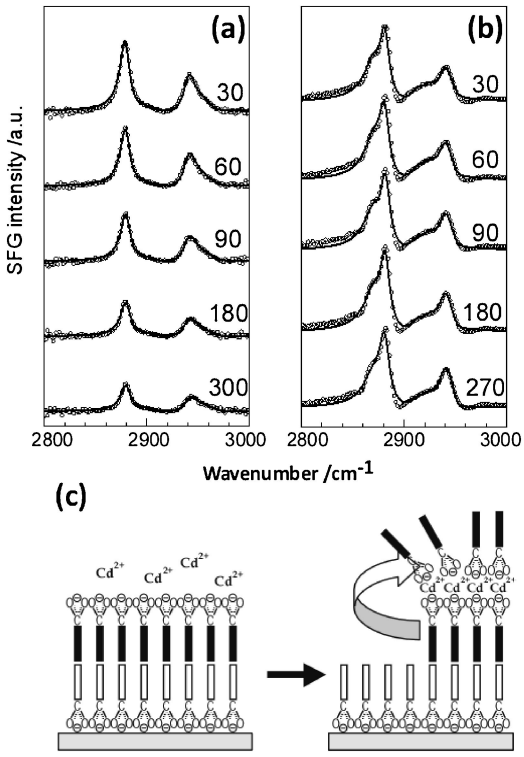

Figure 5. The ssp-polarized SFG spectra of the LB bilayer of deuterated (D) and regular (H) stearate on a fused quartz surface in solutions with (a) 0.2 and (b) 0 mM Cd^{2+} for various immersion times shown in the figure (in min). (c) A schematic model for the structural change of the bilayer induced by Cd^{2+}. Reprint with permission from ref 13, Copyright American Chemical Society.

It is also interesting to know how SFG spectra will be when several interfaces are present in the system. Figure 4 gives such an example, where LB films of $(DH)_n(DD)_mD$ ($n = 1, 2, 3,$ or 4, and $m + n = 4$) on gold substrates were evaluated in the C–H stretching region.[17] In the model system, n DH bilayers with their CH_3 groups pointing toward the substrate (indicated by arrows in inset of Figure 4a) are consciously introduced to provide n SFG-active hetero interfaces in the C–H stretching region. The three peaks can be attributed to C–H stretching resonances of the terminal CH_3 groups in the H layers. The H layers in the multilayers show upward pointing peaks, similar to that of SFG spectrum (a) in Figure 3. The SFG intensity increases with the numbers of DH hetero interfaces. More quantitatively, as shown in Figure 4b, the SFG intensities are almost proportional to n on gold (squares), while they are proportional to n^2 on fused quartz (circles).

The n^2 dependence on fused quartz is easily predicted from eq 1 by neglecting the resonance background. On the other hand, the n dependence on gold is explained by taking into account the interference from the nonresonant background.[17] Note that the results shown above are for the multilayer systems with a thickness much smaller than the wavelength of visible light. For thicker films, an additional optical interference effect arising from multiple reflection of light within the films also should be taken into account.[16]

In Situ Investigation in Solution with ATR Geometry

Although IR spectroscopy has the sensitivity to detect monolayers on metallic surfaces, its application to low reflective surfaces is difficult. On the other hand, SFG can be applied easily to transparent surfaces as well. Figure 5 shows such an example. The samples used here were bilayers prepared by successively depositing deuterated and normal stearate on the flat plane of a hemicylindrical fused quartz prism (which is transparent in both visible and IR). To examine the biyalers in solution, both visible and IR beams were introduced from the prism side in the attenuated total reflection (ATR) geometry (see Figure 2), by which the strong absorption of IR by water can be avoided. In addition, the sensitivity of SFG is significantly enhanced in the ATR geometry.

Figure 5a represents ssp-polarized SFG spectra in the C–H stretching region of the D/H bilayer on a fused quartz surface in an aqueous solution containing 0.2 mM Cd^{2+} (pH 6.7). The bilayer is asymmetric, and hence two intense peaks assigned to the symmetric and Fermi resonance C–H stretching modes of the terminal CH_3 groups in the top H layer are observed (the asymmetric CH stretching mode of CH_3 is weak for ssp polarization). An interesting finding in this figure is that the peaks become weaker with time, which implies some changes in molecular arrangement. A possible interpretation of the result is the partial flip of molecules in the topmost layer to form a HH bilayer on the underlying D monolayer, as schematically illustrated in Figure 5c. The HH bilayer is SFG-inactive, and hence the flip reduces the SFG signals. This interpretation was supported by AFM observation of the bilayer, where many steps with two-

monolayer height were observed on the surface. On the other hand, such a phase transition of the top layer hardly occurs when Cd^{2+} is absent in the solution, as can be found in Figure 5b. This observation suggests that the flip is induced by Cd^{2+} through strong electrostatic interaction of the carboxylate group with Cd^{2+} as shown in Figure 5c. Such a phase transition is difficult to probe by conventional IR and Raman spectroscopy.

Structure of Water at Solid–Solution Interfaces

Water at interfaces plays important roles in many fields of science, especially in electrochemistry, catalysis, micelle formation, and biological processes such as membrane stability and protein activity and hence has been a subject of extensive studies. Shen et al. were the first who investigated structures of water at air/water and water/solution interfaces by SFG spectroscopy.[18–20] Since this pioneering work, the high potential of SFG spectroscopy has came to be widely recognized as a powerful tool for understanding the structures of water at interfaces.

Shen et al. observed that the SFG spectrum of water at a water/fused quartz interface in the OH stretch region is greatly affected by the pH of the solution as shown in Figure 6[19] (Although improved spectra were reported recently,[21] the first reported spectra are shown as a milestone of SFG study). These spectra are characterized by two peaks around 3400 and 3200 cm^{-1}. At very low and high pH, the SFG spectrum (Figures 6a and 6e, respectively) resembles that of ice (Figure 6f) and the peak at 3200 cm^{-1} is dominant, indicating that the interfacial water molecules are ordered like ice (icelike water). On the other hand, the peak around 3400 cm^{-1}, ascribed to hydrogen-bonded OH stretches in a disordered structure (liquidlike water), is significantly developed at intermediate pH (Figures 6b–6d).

The pH dependence was interpreted in terms of acid–base equilibrium of silanol groups on the quartz surface ($Si–OH \leftrightarrow Si–O^- + H^+$). The shift in the acid–base equilibrium changes the hydrogen bonding between water and the surface. In addition, deprotonation of silanol generates a strong electric field at the interface (i.e., electric double layer). As is well known in electrochemistry, water molecules are forced to align to direct their dipole moments along the electrostatic field. When the solution pH is sufficiently low, the surface is terminated by OH groups and the hydrogen-bonding forces water molecules to orient with their dipole moments pointing toward the solution (with O pointing to the surface). At high solution pH, the quartz surface is negatively charged, and the electric field forces water to orient reversely (with O pointing away from the surface). The stronger SFG signal at high pH than at low pH suggests that the electric field orients more water molecules. The opposite orientations of surface water molecules for low and high pH values have been confirmed by phase-sensitive SFG measurements.[22]

For intermediate pH values (Figures 6b–6d), hydrogen bonding and the surface electric field, which have opposite effects on water orientation, are comparable and cause disordering in the interfacial water structure, as seen from the prominent appearance of the 3400 cm^{-1} peak in the spectra.

The structure of water is greatly affected by the nature of the solid surface, as mentioned above. When a fused quartz surface is modified by an octadecyltrichlorosilane (OTS) monolayer,[23] in addition to two hydrogen-bonded OH peaks around 3200 and 3400 cm^{-1}, a sharp peak at 3680 cm^{-1} is observed in neutral

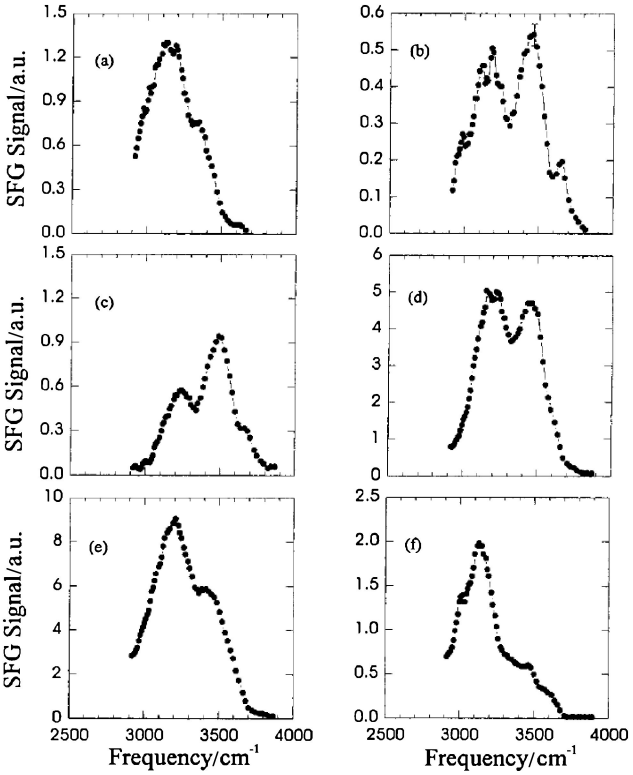

Figure 6. SFG spectra for quartz/water interfaces with different pH values of bulk water: (a) pH 1.5; (b) pH 3.8; (c) pH 5.6; (d) pH 8.0; and (e) pH 12.3. The spectrum for the quartz/ice interface (f) is also shown for comparison. The polarization combination is ssp. Reprint with permission from ref 18, Copyright American Physics Society.

solution. The very high frequency of the peak at 3680 cm^{-1} shows the presence of "free OH" (water molecules without hydrogen bonding). The free OH band has also been observed at water/air interfaces (dangling OH directed toward air),[18–20] hydrophobic interfaces such as dehydrated oxide surface,[24,25] and the water/platinum surfaces covered by carbon monoxide (by IR).[26] The "liquidlike" peak was significantly suppressed in comparison with quartz/water interfaces, indicating that the highly hydrophobic nature of the OTS monolayer can induce a well ordered water layer.

The spectrum of water on a quartz surface modified with an OTS monolayer also strongly depends on pH of the solution,[27] indicating many unreacted silanol groups are still present on the quartz surface after the silane coupling reaction of OTS. The observed spectrum was interpreted as the signals from two different kinds of water molecules, i.e., one located on top of the OTS monolayer and the other located at the OTS/quartz interface are superposed. Similar results have also been obtained on a fused quartz surface modified by different monolayers in aqueous solutions.[27,28]

SFG methods have been also used to study water structures on electrode/solution interfaces.[29–32]

Applications to Biointerfaces

Recently the application of SFG to biochemistry has been increasing. Surface structures of many biopolymers[7] and biomembrane systems[33–38] have been analyzed. For example, the

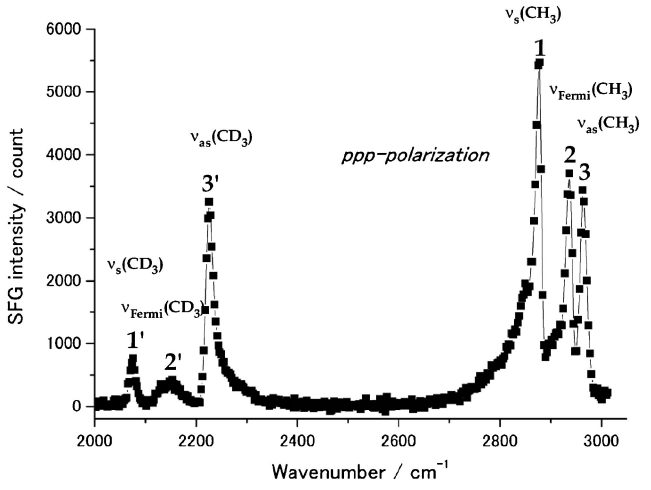

Figure 7. A ppp-polarized SFG spectrum of DPPC/*d*-DPPC bilayer on a CaF_2 substrate in pure water.

surface of poly(2-methoxyethyl acrylate) (PMEA)[39] was examined to find the origin of its excellent compatibility with blood.[40,41] The C=O stretching mode of the carbonyl group on the PMEA surface, observed at 1740 cm^{-1} in air, was found to be shifted to 1722 cm^{-1} after contact with water, while such shift was not observed in bulk PMEA film by conventional IR spectroscopy.[41] The shift is apparently ascribed to the hydrogen bonding between water with the carbonyl group on the PMEA surface. Since this kind of surface hydrogen bond was not observed on similar polyacrylate polymers such as poly(methyl methacrylate) (PMMA) and poly(butyl methacrylate) (PBMA) that do not show such good blood compatibility, the hydrogen bonding on the PMEA surface should play an important role in blood compatibility.

As a model system for biomembranes, Figure 7 shows the SFG spectrum of an asymmetric lipid bilayer composed of dipalmitoylphosphatidylcholine (DPPC, first layer) and deuterated DPPC (second layer), on a CaF_2 substrate in water. In the C–H stretching region (2800–3000 cm^{-1}), three intense peaks assigned to the C–H symmetric (Peak 1), Fermi resonance (Peak 2), and C–H asymmetric stretching (Peak 3) modes from the terminal CH_3 group in the first DPPC layer are observed. In the C–D stretching region (2000–2350 cm^{-1}), the corresponding three C–D stretching peaks, Peaks 1′, 2′, and 3′, can be observed. Peaks from CH_2 and CD_2 groups are very weak, confirming that the alkyl chains of the both DPPC and *d*-DPPC layers take all-trans conformations. It is worth noting that Peak 1 has a tail toward lower frequency and that Peak 3′ has a tail toward high frequency. When the bilayer was made in a reversed sequence, the tail for C–H stretching region appeared in higher frequency region and that for C–D stretching region appeared in lower frequency region (spectrum not shown). Taking into account the orientations of DPPC and *d*-DPPC in the bilayer, the tailing toward different directions can be related to reverse orientations. The tailing is ascribed to the interference from the weak nonresonant signal from CaF_2 substrate.

SFG was also employed to study temperature-induced phase-transition behaviors of lipid bilayers on solid substrates. Liu and Conboy clearly showed the flip–flop processes in different lipid bilayers by using an ns SFG system and evaluated the rate constants of the flip–flop.[33,34] They also determined phase-transition temperatures (T_m) from the temperature dependence of the SFG spectra. By taking the multichannel advantage of a broadband SFG system, our group is focusing on the structural changes during the flip–flop and phase-transition processes.[14] This research is expected to get valuable structural information on biomembranes under a dye-free condition which is widely used in the present stage.

♦ Summary and Future Directions

As shown above, SFG can provide valuable and unique information on molecular structures at surfaces and interfaces. Its advantages over linear vibrational spectroscopy can be summarized as follows; (1) high surface/interface selectivity, (2) monolayer or submonolayer sensitivity, (3) sensitivity to symmetry and ordering, and (4) versatile applicability. Despite the advantages, its applications are still limited compared with other surface analytical techniques. Possible reasons for the limited applications are the very high cost of the instrument and technical difficulties, but these problems will be overcome in the future.

Although the theoretical background of SFG has already been established, SFG processes are complicated and we often encounter difficulties in interpreting observed spectra. Simple explanation of SFG spectra based on linear spectroscopy can lead to mistakes. One way to avoid misinterpretation is detailed theoretical analysis of obtained spectra. A fruitful combination of experimental and theoretical work has been demonstrated in the study of water structures at interfaces.[8,9,42,43] The other way is the combination with other techniques including IR and Raman spectroscopy, by which a comprehensive understanding on the relation between the surface structures and reactivity/functionality will be given. This approach is also useful for quantitative analysis because SFG signals are significantly affected by the local symmetry and interference from the interface and, hence, not always proportional to the number of molecules. Recently, Tyrode et al. coupled SFG and total internal reflection Raman scattering to study the adsorption of hexadecyltrimethylammonium bromide (CTAB) to a silica surface.[44] These two complementary techniques permitted a comprehensive evaluation of the CTAB adlayer structures.

Finally, several new research trends in SFG are noted. First is double-resonance SFG measurements using tunable IR and visible pulses, by which the sensitivity of SFG can be significantly enhanced.[45–49] This is extremely useful to study tiny amounts of chiral molecules in biological systems. Second is SFG imaging which is a promising method to understand the spatial heterogeneities during chemical reaction with high sensitivity.[50,51] The last is the study of ultrafast reaction kinetics and dynamics on the surface or interface which is allowed by using ultrashort pulses in recording SFG.[52–54]

This research was supported by PRESTO, Japan Science and Technology Agency (JST), and Grant-in-Aid for Scientific Research (B) No. 19350099 and for Scientific Research on Priority Area “Strong Photon-Molecule Coupling Fields (No. 470) from MEXT.

References and Notes

1 Z.-Q. Tian, B. Ren, J. Li, Z. Yang, *Chem. Commun.* **2007**, 3514.

2 M. Osawa, *Bull. Chem. Soc. Jpn.* **1997**, *70*, 2861.
3 Y. R. Shen, *The Principles of Nonlinear Optics*, John Wiley & Sons, Inc., New York, **1984**.
4 P. Miranda, Y. R. Shen, *J. Phys. Chem. B* **1999**, *103*, 3292.
5 C. D. Bain, *J. Chem. Soc., Faraday Trans.* **1995**, *91*, 1281.
6 A. Tadjeddine, A. Peremans, in *Spectroscopy for Surface Science*, ed. by R. J. H. Clark, R. E. Hester, Wiley & Sons Ltd, Chichester, UK, **1998**, p. 159.
7 Z. Chen, Y. R. Shen, G. A. Somorjai, *Annu. Rev. Phys. Chem.* **2002**, *53*, 437.
8 G. L. Richmond, *Chem. Rev.* **2002**, *102*, 2693.
9 Y. R. Shen, V. Ostroverkhov, *Chem. Rev.* **2006**, *106*, 1140.
10 S. Ye, K. Uosaki, in *Encyclopedia of Electrochemistry*, ed. by A. J. Bard, Wiley-VCH, Weinheim, **2007**, Vol. 10, p. 513.
11 L. Richter, T. Petralli-Mallow, J. Stephenson, *Opt. Lett.* **1998**, *23*, 1594.
12 S. Ye, H. Noda, S. Morita, K. Uosaki, M. Osawa, *Langmuir* **2003**, *19*, 2238.
13 S. Ye, H. Noda, T. Nishida, S. Morita, M. Osawa, *Langmuir* **2004**, *20*, 357.
14 S. Ye, Y. Tong, M. Osawa, to be submitted.
15 Y. R. Shen, *Proc. Natl. Acad. Sci. U.S.A.* **1996**, *93*, 12104.
16 J. Holman, P. B. Davies, T. Nishida, S. Ye, D. J. Neivandt, *J. Phys. Chem. B* **2005**, *109*, 18723.
17 T. Nishida, C. M. Johnson, J. Holman, M. Osawa, P. B. Davies, S. Ye, *Phys. Rev. Lett.* **2006**, *96*, 77402.
18 Q. Du, R. Superfine, E. Freysz, Y. R. Shen, *Phys. Rev. Lett.* **1993**, *70*, 2313.
19 Q. Du, E. Freysz, Y. R. Shen, *Phys. Rev. Lett.* **1994**, *72*, 238.
20 Q. Du, E. Freysz, Y. R. Shen, *Science* **1994**, *264*, 826.
21 V. Ostroverkhov, G. A. Waychunas, Y. R. Shen, *Chem. Phys. Lett.* **2004**, *386*, 144.
22 Y. R. Shen, *Solid State Commun.* **1998**, *108*, 399.
23 J. Sagiv, *J. Am. Chem. Soc.* **1980**, *102*, 92.
24 D. Liu, G. Ma, H. C. Allen, *Environ. Sci. Technol.* **2005**, *39*, 2025.
25 D. Liu, G. Ma, M. Xu, H. C. Allen, *Environ. Sci. Technol.* **2005**, *39*, 206.
26 M. Osawa, M. Tsushima, H. Mogami, G. Samjeske, A. Yamakata, *J. Phys. Chem. C* **2008**, *112*, 4248.
27 S. Ye, S. Nihonyanagi, K. Uosaki, *Phys. Chem. Chem. Phys.* **2001**, *3*, 3463.
28 S. Nihonyanagi, S. Ye, K. Uosaki, *Electrochim. Acta* **2001**, *46*, 3057.
29 S. Nihonyanagi, S. Ye, K. Uosaki, L. Dreesen, C. Humbert, P. Thiry, A. Peremans, *Surf. Sci.* **2004**, *573*, 11.
30 Z. Schultz, S. Shaw, A. Gewirth, *J. Am. Chem. Soc.* **2005**, *127*, 15916.
31 K. A. Friedrich, W. Daum, F. Dederichs, W. Akemann, *Z. Phys. Chem.* **2003**, *217*, 527.
32 H. Noguchi, T. Okada, K. Uosaki, *Faraday Discuss.* **2009**, *140*, 125.
33 J. Liu, J. C. Conboy, *J. Am. Chem. Soc.* **2004**, *126*, 8894.
34 J. Liu, J. C. Conboy, *J. Am. Chem. Soc.* **2004**, *126*, 8376.
35 X. Chen, H. Tang, M. A. Even, J. Wang, G. N. Tew, Z. Chen, *J. Am. Chem. Soc.* **2006**, *128*, 2711.
36 X. Chen, J. Wang, C. B. Kristalyn, Z. Chen, *Biophys. J.* **2007**, *93*, 866.
37 N. Anderson, L. Richter, J. Stephenson, K. Briggman, *J. Am. Chem. Soc.* **2007**, *129*, 2094.
38 C. Ohe, Y. Goto, M. Noi, M. Arai, H. Kamijo, K. Itoh, *J. Phys. Chem. B* **2007**, *111*, 1693.
39 M. Tanaka, A. Mochizuki, N. Ishii, T. Motomura, T. Hatakeyama, *Biomacromolecules* **2002**, *3*, 36.
40 S. Ye, S. Morita, G. Li, H. Noda, M. Tanaka, K. Uosaki, M. Osawa, *Macromolecules* **2003**, *36*, 5694.
41 G. Li, S. Ye, S. Morita, T. Nishida, M. Osawa, *J. Am. Chem. Soc.* **2004**, *126*, 12198.
42 Papers in *Faraday Discuss.* **2009**, *141*, 1.
43 A. Morita, J. T. Hynes, *Chem. Phys.* **2000**, *258*, 371.
44 E. Tyrode, M. W. Rutland, C. D. Bain, *J. Am. Chem. Soc.* **2008**, *130*, 17434.
45 M. A. Belkin, Y.-R. Shen, *Phys. Rev. Lett.* **2003**, *91*, 213907.
46 N. Ji, Y. R. Shen, *Chirality* **2006**, *18*, 146.
47 T. Ishibashi, H. Onishi, *Chem. Lett.* **2004**, *33*, 1404.
48 T. Maeda, T. Ishibashi, *Appl. Spectrosc.* **2007**, *61*, 459.
49 Q. Li, R. Hua, K. C. Chou, *J. Phys. Chem. B* **2008**, *112*, 2315.
50 S. Baldelli, *ChemPhysChem* **2008**, *9*, 2291.
51 Y. Zhang, Y. Tong, M. Abe, K. Uosaki, M. Osawa, Y. Sasaki, S. Ye, *J. Mater. Chem.* **2009**, *19*, 261.
52 C. Matranga, P. Guyot-Sionnest, *J. Chem. Phys.* **2000**, *112*, 7615.
53 H. Noguchi, T. Okada, K. Uosaki, *J. Phys. Chem. B* **2006**, *110*, 15055.
54 A. Bandara, J. Kubota, K. Onda, A. Wada, S. S. Kano, K. Domen, C. Hirose, *J. Phys. Chem. B* **1998**, *102*, 5951.